Springer

KSME

Journal of Mechanical Science and Technology 27 (8) (2013) 2467~2476
www.springerlink.com/content/1738-494x
DOI 10.1007/s12206-013-0632-7

Experimental modeling and multi-objective optimization of traveling wire electro-chemical spark machining (TW-ECSM) process †

Basanta Kumar Bhuyan* and Vinod Yadava

Mechanical Engineering Department, Motilal Nehru National Institute of Technology Allahabad, Allahabad-211004, India

(Manuscript Received October 18, 2012; Revised January 10, 2013; Accepted February 19, 2013)

Abstract

The present paper attempts to focus an application of a hybrid methodology comprising of Taguchi methodology (TM) coupled with response surface methodology (RSM) for modeling and TM coupled with weighted principal component (WPC) methodology for multi-objective optimization of a self developed traveling wire electro-chemical spark machining (TW-ECSM) process. First optimum level of input parameters is found using TM which is used as the central values in RSM to develop the second-order response model. For multi-objective optimization two quality characteristics surface roughness (R_a) and material removal rate (MRR), which are of opposite nature (R_a is the lower-the-better type, while MRR is the higher-the-better type), have been selected. The WPC is employed for the calculation of weight corresponding to each quality characteristic. The results indicate that the hybrid approaches applied for modeling and optimization of the TW-ECSM process are reasonable.

Keywords: MRR; R_a; Response surface methodology; Traveling wire electro-chemical spark machining; Taguchi methodology; Weighted principal component

1. Introduction

In recent years, aerospace industries and modern defense industries demand that their highly sophisticated products are developed in the route of high precision, high speed, high temperature, high pressure, and large power. The materials used in these products are mainly glasses, ceramics, and composites. Borosilicate glass is becoming more important for such type of products due to its improved strength, thermal resistance, and corrosion resistance. It has wide applications in micro-electromechanical systems (MEMS).

Due to the high material hardness and brittleness, borosilicate glass has been found as one of the material which is difficult-to-machine using conventional or unconventional machining methods. Ultrasonic machining (USM), abrasive jet machining (AJM), laser beam machining (LBM), and electron beam machining (EBM) are some of the unconventional machining processes that can be used for machining these materials, but dimensional accuracy and surface quality of the machined surfaces are the major concerns. Therefore, researchers have been focused on developing several combinations of different machining processes known as hybrid machining processes (HMPs) for machining these materials. HMPs can be defined as an enhanced material removal process that can achieve a considerably better machining effect or extended machining ability by combining at least two of the thermal, chemical, electrochemical, magnetic, or mechanical effects to upgrade the ability of workpiece material removal or to promote the removal of machining products from the machining gap. These processes also attempt to satisfy the increasing challenges posed by advanced difficult-to-machine materials and related complex and accurate shapes. HMPs are developed to exploit the superiority of each of the constituent machining process and diminish the inferiority of each constituent process. It also reduces some adverse effects of the constituent processes while they are applied individually. Recently, a new spark based machining method has been found an effective machining method suitable for machining of such type of hard and brittle electrically non-conducting materials. This new machining process combines the features of electro chemical machining (ECM) and electro discharge machining (EDM) and called as electro-chemical spark machining (ECSM) method.

The ECSM process uses electro-chemical discharge (ECD) phenomenon for generating heat for the purpose of removing work material by melting and vaporization. This was presented for the first time by Kurafuji as "electrochemical discharge drilling (ECDD)" for creating microholes in glass workpiece [1]. Several other names of ECSM are used in literature by different researchers, such as electro chemical arc

*Corresponding author. Tel.: +91 5322271726, Fax.: +91 5322445077
E-mail address: bkbhuyan@mnnit.ac.in
† Recommended by Associate Editor Ki-Hoon Shin

machining (ECAM), electro chemical discharge machining (ECDM) and spark assisted chemical engraving (SACE) [2]. ECSM process has been tried in many configurations, such as die Sinking-ECSM, hole sinking-ECSM, die drilling-ECSM, hole drilling-ECSM, wire cutting-ECSM, disc cutting-ECSM, cylindrical grinding-ECSM, surface grinding-ECSM, and pocket milling-ECSM. Die sinking-ECSM operation usually involves machining of cavity of small depth to diameter ratio using non-rotating tool electrode, but in hole drilling-ECSM a rotating tool electrode is used to make large depth to diameter symmetrical holes. Wire cutting-ECSM is capable of slicing large volumes and machining complex shapes of non-conducting materials without the need of full form tool electrode. In contour milling-ECSM, a simple shape tool electrode is used to produce a three-dimensional (3-D) cavity by adapting a movement strategy similar to conventional milling. Success in the application of sinking and drilling ECSM has stimulated interest in studying the prospects of TW-ECSM.

In 1985, Tsuchiya et al. [3] developed TW-ECSM setup first time for cutting non-conducting materials such as glasses and ceramics. After its inception, many researchers have given attention for the experimental study of ECSM process to make it industrially viable process for cutting non-conducting workpiece materials. The discharge phenomenon during ECSM has been studied by many researchers [4]. Hofy and McGeough [5] experimentally studied the effect of mode of electrolyte flushing on metal removal rate during wire electrochemical arc machining (WECAM) of rectangular mild steel plate and recommended that the use of coaxial mode of flushing is better from machining action and accuracy point of view. Peng and Liao [6] claimed that TW-ECDM can be applied for slicing of meso-size non-conductive brittle materials such as quartz bar and borosilicate optical glass of several mm thickness. They also verified that pulsed DC power shows better spark stability and more spark energy than constant DC power. Nesarikar et al. [7] used TW-ECSM process for precision slicing of thick Kevlar-epoxy composite. They did a comparison between the experimental and calculated values of MRR and average diametral over-cut with the variations in electrolyte conductivity, applied voltage and specimen thickness. Jain et al. [8] conducted experiments on their self developed setup of TW-ECSM for cutting glass epoxy and Kevlar epoxy composites using NaOH electrolyte. They reported that higher MRR can be achieved at higher voltage with the presence of large thermal cracks, large HAZ and irregular machined surfaces. Yang et al. [9] conducted experimental study during TW-ECDM to improve the over-cut quality by adding SiC abrasive particles to the electrolyte. They have also reported the effect of adding abrasives on surface roughness (R_a) and MRR due to TW-ECDM. Singh et al. [10] have reported the feasibility of using TW-ECSM process for machining of electrically partially conductive materials like piezo-electric ceramics (PZT) and carbon fiber epoxy composites. They observed that MRR increases with increase in supply voltage and also increases with increase in concentration of the electrolyte upto around 20% wt. beyond this concentration, it starts decreasing.

Different hybrid mathematical approaches have recently been used for the optimization of different machining processes. Taguchi method with fuzzy logic (FL) [11] or with grey relational analysis (GRA) [12] has been used to optimize the EDM process with multiple objective machining performances. Sharma and Yadava [13] have suggested the use of a hybrid approach TMRSM for modeling comprising of TM and RSM and also the use of TMGRA comprising TM and GRA methodology for multi-objective optimization of pulsed Nd:YAG laser cutting process. The hybrid approach TMRSM and TMWPC have yet not been applied in the study of TW-ECSM process with single or multiple performance measures.

In this paper, two different hybrid approaches have been applied, one is used for modeling and another for multi-objective optimization during TW-ECSM process. First hybrid approach which comprises of TM and RSM is called as TMRSM and the second is known as TMWPC which couples TM with WPC. R_a and MRR have been considered as performance characteristics. In TMRSM, initially the optimum process parameters have been determined for multiple quality characteristics using TM only. Firstly, TM is used to determine the level of input parameters corresponding to minimum R_a and maximum MRR. These levels of input parameters are further used as a central value in the design of central composite rotatable design (CCRD) matrix. Finally, second-order response surface models are developed for R_a and MRR after conducting experiments using CCRD matrix [14]. An attempt has also been made to carry out optimal parametric analysis on TW-ECSM process, to achieve better control for a quality cut. Further, TMWPC approach has been applied for multi-objective optimization of the process where experimental results have been used in weighted principal component for finding the normalized quality characteristics and data summary of the multi-response performance index (MPI). Taguchi-based L_9 orthogonal array (OA) was selected for performing the experiments and the weighted principal component is specially employed to calculate the weight of each quality characteristic.

2. Experimental procedure and operating parameters

The experimental studies were performed on self developed traveling wire electro-chemical spark machining (TW-ECSM). Fig. 1 shows the (a) schematic diagram and (b) the real photographic view of the experimental setup. The variable input process parameters (control factors) taken are voltage, electrolyte concentration, wire feed velocity and workpiece thickness. An exhaustive pilot experiment was conducted to decide the parameter range for a quality cut. In experiments, graphite rod (diameter 8 mm, length 55 mm) was used as anode and brass wire of diameter 0.25 mm was used as cathode. A rectangular borosilicate glass of size 40 mm × 35 mm × 2 mm was adopted as a workpiece and material properties of workpiece

Table 1. Properties of borosilicate glass (80.6%SiO_2, 13.0%B_2O_3, 4.0%N_2O, and 2.3% Al_2O_3).

C_p (J/Kg ºC)	750
k (W/m ºC)	1.14
T_m (ºC)	820
ρ (kg/m^3)	2,230

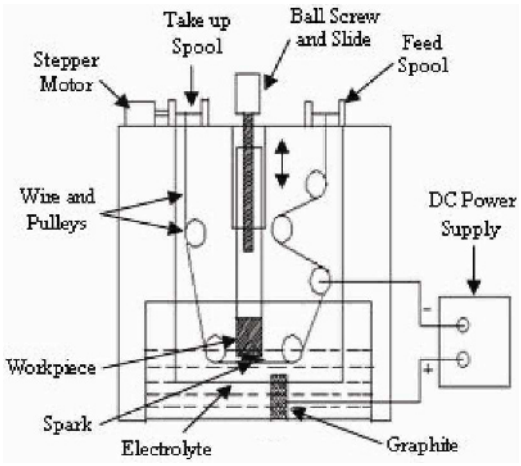

(a)

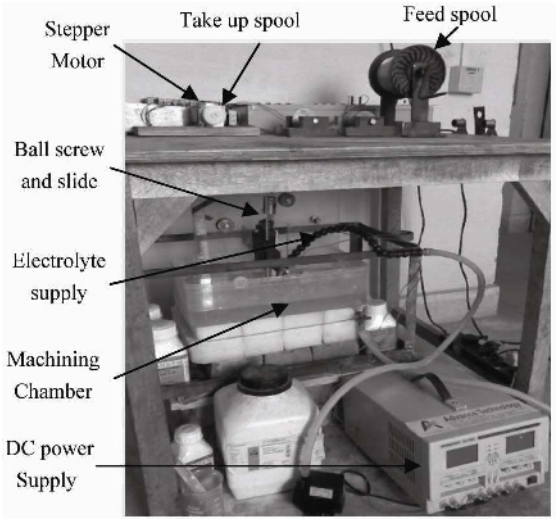

(b)

Fig. 1. (a) Schematic diagram; (b) Photographic view of the developed tabletop TW-ECSM setup.

are given in Table 1.

Workpiece was held at constant distance of about 45 mm from the anode. Cathode (wire) was always kept in physical contact with the workpiece which was mounted on the supporting platform. Brass wire was broken at above 65 volts because of its low current carrying capacity. Hence, voltage was decided with the range of 40 V-65 V. Very low wire speed would lead to the situation similar to the stationary tool resulting in overheating and finally breaking of the wire. Too high wire speed was also not desirable because it would be uneconomical. Hence, wire was driven by stepper motor with a range of 0.6-4 m/min. NaOH has higher specific conductance, reactions take place at higher rates, so a larger amount of gases were evolved. Hence, higher MRR was achieved. Thus, all the experiments reported in this paper were carried out using NaOH solution as electrolyte. An aqueous solution of NaOH with a range of 150 g/l to 350 g/l solution at 20ºC to 40ºC was used. Each experiment was tested for about 10 to 15 min., during which voltage and current were recorded on a voltmeter and ammeter, respectively.

Table 2. Control factors and their levels.

Symbol	Input parameters	Units	Level 1	Level 2	Level 3
A	Voltage	volt	45	50	55
B	Electrolyte concentration	g/l	150	200	250
C	Wire feed velocity	m/min	1.8	2.4	3
D	Workpiece thickness	mm	3	4	5

The minimum linear feed rate to the workpiece which could be achieved using the present setup was 0.008 mm/s. This feed rate was higher than the cutting rate observed during the experiments. The pulsating DC power supply has been used during the experiments due to better spark stability and more spark energy than constant DC power. Hence, experiments carried out using constant pulse on time of 0.2 ms and pulse off time of 0.4 ms respectively. The numerical values of factors at different levels are shown in Table 2. The two quality characteristics analysed are R_a and MRR. For evaluation of MRR, the loss in weight of the machined specimen was measured on a weighing digital microbalance (accuracy 10 µg, CAS India Private Limited). After machining, the workpiece was washed, dried to evaporate any water remaining on the surface and reweighed using a weighing digital micro balance. The difference between the initial weight and the final weight was given the amount of material removed. The R_a value was measured using a surface roughness tester (SURTRONIC-25 model, Taylor Hobson Ltd., UK). The initial setting of input parameters is voltage (45V), electrolyte concentration (150 g/l), wire feed velocity (1.8 m/min) and workpiece thickness (3 mm). Now, the four parameters at three different levels assuming no interaction between factors, the degree of freedom (DOF) has been calculated as (3-1) × 4+1=9 [15]. Hence, a standard L_9 OA has been selected for the experimental design matrix as shown in Table 3.

3. Modeling of TW-ECSM using TMRSM

In the present work, lower values of R_a and higher values of MRR are desirable. These characteristics in the Taguchi methodology are termed as the lower-the-better (LB) type and higher-the-better (HB) type characteristics. Mathematically, the S/N ratios for LB and HB type quality characteristics are

computed as [15, 16]:

$$\eta = -10\log10\ (MSD) \tag{1}$$

where, MSD = mean square deviation or quality loss function is used to calculate the deviation between the experimental value and the desired value.

$$\text{For LB type, MSD}=\left[\frac{1}{n}\sum_{i=1}^{n} y_i^2\right] \tag{2}$$

$$\text{For HB type, MSD}=\left[\frac{1}{n}\sum_{i=1}^{n}\frac{1}{y_i^2}\right] \tag{3}$$

where y_i is the observed data or quality value of the i^{th} trial and n is the number of trial at the same condition of experiment. In multi-objective optimization, a single overall S/N ratio for all quality characteristics is computed instead of separate S/N ratio for each quality characteristic. This overall S/N ratio is known as the name of multiple S/N ratio (MSNR). The MSNR for j^{th} trial (η_j) is calculated as given below [17].

$$\eta_j^e = -10\log10\ (Y_j) \tag{4}$$

$$Y_j = \sum_{i=1}^{p} w_i y_{ij} \tag{5}$$

$$y_{ij} = \frac{L_{ij}}{L_{i^*}} \tag{6}$$

where Y_j is the total normalized quality loss in j^{th} trial, w_i represents the weighting factor for the i^{th} quality characteristic, p is the number of quality characteristics and y_{ij} is the normalized quality loss associated with the i^{th} quality characteristic at j^{th} trial condition and it varies from a minimum of zero to a maximum of one. L_{ij} is the quality loss or MSD for the i^{th} quality characteristic at j^{th} trial and L_{i*} is the maximum quality loss for the i^{th} quality characteristic among all the experimental runs. The quality loss values for different quality characteristics in each experimental run are calculated using Eqs. (2) and (3) (Table 3). The normalized quality loss (NQL), total normalized quality loss (TNQL) and multiple signal-to-noise ratios (MSNR) for multiple quality characteristics R_a and MRR have been calculated using Eqs. (4)-(6). These results are shown in Table 4. Through MINITAB software, the optimal process cutting parameters with several weighting combinations of quality characteristics have been obtained. The value of weighting factor is dependent upon engineering judgment.

The optimum conditions of the cutting parameters for multi-performance outputs with different combinations of the weighting factors as shown in Table 5. As Table 5 clearly demonstrates that the optimum cutting conditions for lower R_a and higher MRR were found in case 1 where high value of w_1 = 0.6 and low value of w_2 = 0.4 were used. In case 2, the cutting conditions were obtained higher as compared to case 1 for R_a and MRR where R_a and MRR have equal weighting factors i.e. $w_1 = w_2 = 0.5$.

The cutting conditions were also found medium results in case 3 as compared to other two cases for R_a and MRR while

Table 3. Experimental observations using L_9 OA and Quality loss for R_a and MRR.

Exp. no.	Factor levels				R_a (μm)	MRR (mm^3/min)	Quality loss (dB)	
	A	B	C	D			R_a	MRR
1	1	1	1	1	4.6	0.1658	21.16	36.3773
2	1	2	2	2	7.4	0.1976	54.76	25.6109
3	1	3	3	3	8.6	0.2481	73.96	16.2460
4	2	1	2	3	11.6	0.2003	134.56	24.9252
5	2	2	3	1	10.4	0.5172	108.16	03.7384
6	2	3	1	2	7.8	0.4932	60.84	04.1111
7	3	1	3	2	12.0	0.2780	144.00	12.9393
8	3	2	1	3	11.2	0.9267	125.44	01.1645
9	3	3	2	1	13.2	1.4289	174.24	00.4898

Table 4. Normalized quality loss (NQL) values for R_a and MRR and Total normalized quality loss (TNQL) and Multiple S/N ratios (MSNR).

Exp. no.	Factor levels				NQL values		TNQL	MSNR (dB)
	A	B	C	D	R_a	MRR		
1	1	1	1	1	0.1214	1.0000	0.4728	3.2532
2	1	2	2	2	0.3143	0.7040	0.4702	3.2772
3	1	3	3	3	0.4245	0.4466	0.4333	3.6321
4	2	1	2	3	0.7723	0.6852	0.7375	1.3224
5	2	2	3	1	0.6208	0.1028	0.4136	3.8342
6	2	3	1	2	0.3492	0.1130	0.2547	5.9397
7	3	1	3	2	0.8264	0.3557	0.6381	1.9511
8	3	2	1	3	0.7199	0.0320	0.4447	3.5193
9	3	3	2	1	1.0000	0.0135	0.6054	2.1796

Table 5. Optimum cutting conditions for R_a and MRR with different weighting factor.

Cutting parameters and performance characteristics	Optimum cutting conditions		
	Case 1 $w_1 = 0.6, w_2 = 0.4$	Case 2 $w_1 = 0.5, w_2 = 0.5$	Case 3 $w_1 = 0.4, w_2 = 0.6$
Voltage	50	50	50
Electrolyte concentration	250	250	250
Wire feed velocity	1.8	1.8	1.8
Workpiece thickness	4	4	4
R_a (μm)	5	5.8	5.6
MRR (mm^3/min)	0.8193	0.8990	0.8712

Table 6. Effect of factor levels on MSNR.

Symbol	Mean of multiple S/N ratios (dB)			
	Control factors	Level 1	Level 2	Level 3
A	Voltage	3.3857	3.6988*	2.5500
B	Electrolyte concentration	2.1756	3.5436	3.9171*
C	Wire feed velocity	4.2374*	2.2597	3.1391
D	Workpiece thickness	3.0890	3.7227*	2.8246

*Optimum parameter level

Table 7. Control factors and their coded levels in CCRD.

Symbol	Control factors	Units	Coded levels				
			-2	-1	0	1	2
A	Voltage	volt	40	45	50	55	60
B	Electrolyte concentration	g/l	150	200	250	300	350
C	Wire feed velocity	m/ min	0.6	1.2	1.8	2.4	3.0
D	Workpiece thickness	mm	2	3	4	5	6

low value of $w_1 = 0.4$ and high value of $w_2 = 0.6$ were used. Therefore, $w_1 = 0.6$ and $w_2 = 0.4$ in case 1 is recommended in this study and also the lower R_a is more important for cutting applications. The effect of various control factors on MSNR is shown in Table 6. The optimum levels of different control factors or input process parameters for minimum R_a and maximum MRR obtained are voltage at level 2 (50 volt), electrolyte concentration at level 3 (250 g/l), wire feed velocity at level 1 (1.8 m/min) and workpiece thickness at level 2 (4 mm). The optimum value of process parameters have further been used in RSM as a central value for CCRD matrix.

In general, a second-order regression model is given below utilized in surface roughness method because first-order models frequently give lack-of-fit [18].

$$y = b_0 + \sum_{i=1}^{p} b_i x_i + \sum_{i=1}^{p} b_{ii} x_i^2 + \sum_i \sum_j b_{ij} x_i x_j \quad (7)$$

where all b's are regression coefficients determined by least square method [18]. In order to estimate the regression coefficients in this model each variable x_i must be taken at least three different levels. It requires 3^p number of experiments in factorial design but this is a tedious work with large number of factors. For fitting second-order model a new design known as central composite design (CCD) is generally used [14]. The control factors, their numerical and coded values used in CCRD matrix are shown in Table 7. In CCRD matrix contains total 31 runs with 2^p factorial runs, 2p axial runs and 7 centre point runs. In present work, number of control factors (p) are 4. Therefore, total number of runs = $2^4+2*4+7 = 31$.

The central value of process parameters corresponding to code '0' is the optimum parameter level obtained from multi-objective optimization using Taguchi method. The value of 'a' in CCRD is calculated as

$$a = (2^p)^{1/4} = 2.$$

Hence, the coded values for different levels in CCRD are -2, -1, 0, 1 and 2. The numerical values assigned to voltage, electrolyte concentration, wire feed velocity and workpiece thickness at different coded levels are so chosen that the range of parameters do not exceed the extreme limits of individual process parameters decided for complete through cutting as observed during pilot experimentations.

The second-order response surface model for R_a and MRR has been developed from the experimental response values obtained using CCRD experimental matrix as shown in Table 8. The model developed using MINITAB software is given below:

$$R_a\,(\mu m) = 7.57143 - 0.7000x_1 + 1.2333x_2 - 0.0833x_3 + 0.4000x_4 + 1.4779x_1^2 + 0.3029x_2^2 + 0.2029x_3^2 + 0.3779x_4^2 + 0.9500x_1x_2 - 1.1750x_1x_3 - 0.1750x_1x_4 - 0.5000x_2x_3 + 0.2000x_2x_4 + 0.3750x_3x_4 \quad (8)$$

$$MRR\,(mm^3/min) = 0.4905 + 0.1641x_1 - 0.0054x_2 + 0.0442x_3 + 0.0081x_4 - 0.0238x_1^2 - 0.0018x_2^2 - 0.0199x_3^2 + 0.0197x_4^2 - 0.0273x_1x_2 + 0.0125x_1x_3 - 0.0126x_1x_4 + 0.0291x_2x_3 + 0.0257x_2x_4 + 0.0239x_3x_4 \quad (9)$$

where x_1 is voltage (Volt), x_2 is electrolyte concentration (g/l), x_3 is wire feed velocity (m/min) and x_4 is workpiece thickness (mm). To test whether the data are well fitted in model or not, the calculated S value of the regression analysis for R_a and MRR are obtained as 2.37335 and 0.059302 respectively, which are smaller and R^2 value for both the responses are 64.04% and 93.33%. The value of R^2 (adj) for R_a and MRR is 32.58% and 87.50% respectively. These are moderately high (except R^2 (adj) for R_a which is moderate) therefore model fits the data. Hence, the data for each response are well fitted in the developed models. Analysis of variance (ANOVA) and subsequently F-ratio test and p-value test have been carried out to test the adequacy of the developed mathematical models for R_a as well as MRR. The Table 9 shows the results of ANOVA, p-value of the source of regression model and linear effects are lower than 0.01 for both the responses. Developed regression model and linear effect of parameters for both the responses are significant. Calculated F-value of the lack-of-fit for R_a and MRR are 3.25 and 5.35 respectively, which are lower than the critical value of the F-distribution 7.87 as found from standard table at 99% confidence level. Therefore, the developed second-order regression model for R_a and MRR are adequate at 99% confidence level.

From the developed models, it is clear that the electrolyte

Table 8. Experimental observations using CCRD.

Exp. no.	Factor levels				R_a (μm)	MRR (mm^3/min)
	A	B	C	D		
1	0	0	0	0	7.8	0.4874
2	-1	1	-1	-1	5.0	0.2381
3	1	1	1	-1	6.4	0.6532
4	1	-1	-1	1	5.8	0.5864
5	1	-1	1	-1	5.2	0.6128
6	-1	-1	-1	1	9.2	0.1978
7	0	0	-2	0	10.4	0.3157
8	0	0	0	0	7.4	0.4962
9	0	0	0	0	8.0	0.4902
10	1	1	1	1	8.6	0.7512
11	0	0	0	2	10.2	0.6329
12	-1	-1	1	1	10.6	0.2438
13	-1	-1	1	-1	11.0	0.2645
14	-1	1	1	-1	12.2	0.2612
15	0	0	2	0	8.2	0.5846
16	-1	1	-1	1	11.6	0.3216
17	-1	1	1	1	13.4	0.3854
18	0	0	0	-2	9.8	0.5841
19	0	0	0	0	7.0	0.4874
20	1	-1	-1	-1	5.4	0.7235
21	-2	0	0	0	14.6	0.1563
22	0	0	0	0	7.8	0.4892
23	-1	-1	-1	-1	10.8	0.2358
24	0	-2	0	0	6.4	0.5782
25	0	0	0	0	8.2	0.4901
26	1	1	-1	1	11.4	0.4725
27	0	0	0	0	6.8	0.4932
28	2	0	0	0	14.2	0.7124
29	0	2	0	0	13.0	0.4671
30	1	1	-1	-1	15.4	0.5246
31	1	-1	1	1	9.6	0.6512

Table 9. Results of ANOVA for developed models.

Source	R_a model		MRR model	
	F-value	*p*-value	*F*-value	*p*-value
Regression	2.04	0.008	16.00	0.000
Linear	2.32	0.001	49.46	0.000
Square	2.86	0.058	2.96	0.052
Interaction	1.30	0.313	2.38	0.077
Lack-of-fit	3.25	0.000	5.35	0.000

concentration, workpiece thickness, square effect of voltage and interaction effect of wire feed velocity and workpiece thickness are the significant factors for R_a, because the absolute value of corresponding coefficients for these terms are quite high in comparison to other terms. Similarly, the MRR is significantly affected by voltage, wire feed velocity, square effect of workpiece thickness and interaction effect of electrolyte concentration and workpiece thickness.

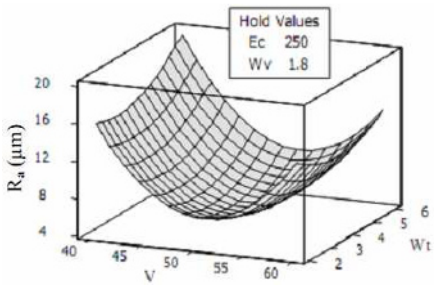

Fig. 2. Response surface plot of R_a with voltage and workpiece thickness.

4. Analysis of the parametric influences

The influences of process parameters (Voltage (V), Electrolyte concentration (Ec), Wire feed velocity (Wv) and Workpiece thickness (Wt)) on R_a and MRR in TW-ECSM are analysed based on the mathematical modeling i.e. Eqs. (8) and (9). All were observed through RSM plot.

4.1 Effect of process parameters on R_a

Based on the non-linear mathematical model of R_a established through RSM, the effect of voltage and workpiece thickness on R_a in TW-ECSM process was observed during cutting of borosilicate glass. The variation of R_a with these process parameters keeping electrolyte concentration and wire feed velocity as a constant value is depicted in Fig. 2. From the graph it can be observed that the R_a decreases initially with voltage upto 50 V and then it starts increase upto 60 V. The nature of the variation of the curve for R_a with respect to voltage is quite similar for the different workpiece thickness.

This is due to the fact that more energy is required to establish the plasma channel which causes a shallow crater on the machined surface and the second part of the curve due to a large number of gas bubbles are generated at the tool (wire) circumference, results more spark which causes deeper crater on the workpiece. In case of workpiece thickness the reason is that the obstruction in the current path resulting in less bubble formation on the wire passing through the groove and the energy generated on the wire away from the workpiece is wasted in heating the electrolyte. Similarly, second part of the curve because of discharge zone in the vicinity of the wire gets shifted to the top of the workpiece and more bubble concentration on the wire passing through the groove resulting higher discharge energy per spark which implies larger value of depth of crater and thus increasing the value of R_a.

Fig. 3 demonstrates the effect of voltage and wire feed velocity on R_a keeping electrolyte concentration and workpiece thickness as a constant value such as 250 g/l and 4 mm respectively. From the surface plot, it has been observed that R_a first

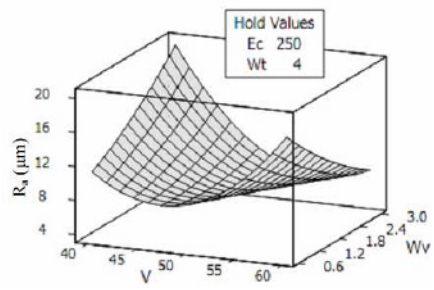

Fig. 3. Response surface plot of R_a with voltage and wire feed velocity.

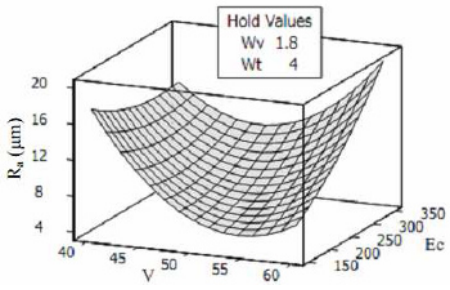

Fig. 4. Response surface plot of R_a with voltage and electrolyte concentration.

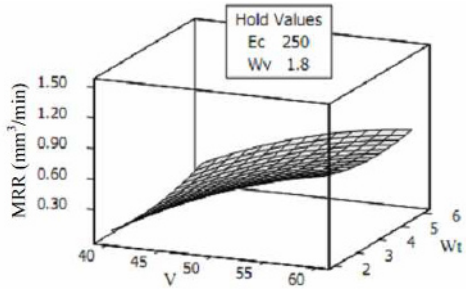

Fig. 5. Response surface plot of MRR with voltage and workpiece thickness.

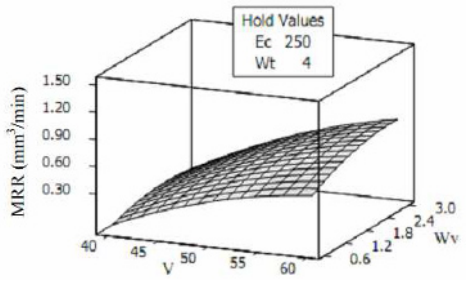

Fig. 6. Response surface plot of MRR with voltage and wire feed velocity.

decreases and then increases gradually in curvilinear manner with change in voltage as well as change in wire feed velocity. At moderate value of wire feed velocity, lower value of R_a has been found by using different levels of voltage. The fact is that at higher wire feed velocity very less bubble formation at the sidewall of the tool, which causes lower crater on the machined surface.

The influences of voltage and electrolyte concentration on R_a are determined based on a second order mathematical model as shown in Fig. 4. Workpiece thickness and wire feed velocity are taken as constant at 4 mm and 1.8 m/min respectively.

From Fig. 4 it is observed that R_a decreases with increase in voltage when electrolyte concentration is kept at lower level. At higher level of electrolyte concentration, R_a increases with the increase of voltage because higher electrolyte concentration means higher specific conductance implies increased electrolyte conductivity which results more circuit current. At higher values of circuit current means more heat energy penetrates into the workpiece and consequently larger value of depth of crater and thus producing higher value of R_a.

4.2 Effect of process parameters on MRR

Keeping electrolyte concentration and wire feed velocity constant at 250 g/l and 1.8 m/min, the effect of voltage and workpiece thickness on MRR is illustrated in Fig. 5. The variation of MRR with the voltage is quite similar to the effect of different workpiece thickness. The MRR during TW-ECSM operation increases with an increase in voltage because of the fact that at high voltage a large number of gas bubbles are generated and accumulated at the tool sidewall, resulting in a large amount of spark generation in the sparking zone which in turn enhances the MRR. The graph also reflects that MRR increases with increase in workpiece thickness because the discharge zone in the vicinity of the wire gets shifted to the top of the workpiece and more bubble concentration take place on the wire passing through the groove resulting in higher discharge energy per spark and thus enhances the value of MRR.

From the surface plot of MRR, the effects of voltage and wire feed velocity at constant electrolyte concentration of 250 g/l and workpiece thickness of 4 mm have been analysed as shown in Fig. 6. The graph depicts that MRR increases with increase in voltage at different wire feed velocity. The value of MRR is higher at 60 V and it continuously increases when the wire feed velocity is gradually increases from 0.6 m/min to 3 m/min keeping the voltage at higher level i.e. 60 V. This occurs due to the higher discharge energy per spark at lower level of wire feed velocity and generation of more number of gas bubbles at higher voltage. Increase in the wire feed velocity implies the electrochemical dissolution condition was gradually covered up by discharge action, as a result of the high current density, resulting in the evolution of abundant amount of hydrogen gas bubbles which promotes discharge.

Therefore, discharge energy per spark increases thereby enhancing the MRR.

Fig. 7 exhibits the effect of voltage and electrolyte concentration on MRR by keeping wire feed velocity and workpiece thickness constant at 1.8 m/min and 4 mm respectively. From the response graph it has been observed that MRR increases linearly with the increase in voltage at different electrolyte

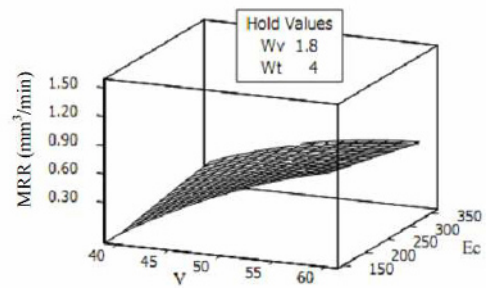

Fig. 7. Response surface plot of MRR with voltage and electrolyte concentration.

concentration. It has also been observed that the MRR increases with increase in electrolyte concentration upto 250 g/l and then it starts to decrease. It occurs due to reduction of the specific conductance of electrolyte after achieving the electrolyte concentration level of 250 g/l which consequently decreases the circuit current. Moreover, the heat energy developed from the spark is proportional to the circuit current and as a result MRR decreases at higher values of concentration.

5. Optimization of TW-ECSM process using TMWPC

The values of R_a and MRR from Table 3 corresponding to each experimental run have been used in WPC for optimization of TW-ECSM process. WPC is one of the most promising approaches [19] for optimization of multi-response processes makes use of all the principal components irrespective of the eigenvalues so that the overall variation in all the responses can be completely explained. In this method, the proportion of overall variation explained by each component is treated as the weight to combine all the principal components in order to form a multi-response performance index (MPI). The best combination of the parametric settings can easily be obtained that can optimize the MPI. The MPI value for ith trial, as computed using the following equation as [20]:

$$MPI^i = \sum_{l=1}^{q} W_l Z_l^i \tag{10}$$

where W_l is the weight of l^{th} principal components, Z_l^i is the computed value of l^{th} principal component corresponding to i^{th} trial. Here, the additive model is appropriate because all the principal components are independent of each other. The larger value of MPI will imply the better quality. Finally, with the application of ANOVA, significant factors in this quality index and their contribution percentage for total variation in MPI will be obtained.

In present case, the desired responses were (a) R_a (lower-the-better type) and (b) MRR (higher-the-better type) and the experimentation considering three levels for all control factors. Therefore, the standard L_9 OA was used for the experiments and same experimental values were also applied to determine the optimal parametric settings using WPC method. For this purpose, quality loses were computed and transformed into normalized quality loss values for each response variable for all the 9 trials (Tables 3 and 4). Here, it is shown that two principal components are obtained with the proposed WPC method to revise principal component analysis (PCA). Hence, Table 10 shows the explained variation in these two responses and the eigenvector of each principal component. The relations between principal components and responses are [19]:

Z_1=0.707×R_a + 0.707×MRR and
Z_2=-0.707×R_a + 0.707×MRR

where Z_1 is the first principal component and Z_2 is the second principal component. The MPI value can be computed using the Eq. 10 as given below:

MPI=0.7954×Z_1+0.2047×Z_2.

Table 11 shows the obtained MPI value in the standard orthogonal array L_9 and Table 12 shows the calculation results in computing the main effect of each controllable factor's levels. It is clearly evident that the best combination of factors/levels is obtained as $A_1B_1C_2D_3$ and Fig. 8 shows the response graph for MPI. Analysis of variance is a computational technique to

Table 10. Effect of factor levels on MPI.

Principal components	Eigenvalue	Explained variation (%)	Cumulative variation (%)	Eigenvector [R_a and MRR]
Z_1	1.5907	79.54	79.54	[0.7071, 0.7071]
Z_2	0.4093	20.46	100.00	[-0.7071, 0.7071]

Table 11. Data summary of the MPI.

Exp. no.	A	B	C	D	MPI
1	1	1	1	1	0.7577
2	1	2	2	2	0.6290
3	1	3	3	3	0.4931
4	2	1	2	3	0.8071
5	2	2	3	1	0.3319
6	2	3	1	2	0.2259
7	3	1	3	2	0.5966
8	3	2	1	3	0.3233
9	3	3	2	1	0.4271

Table 12. Effect of factor levels on MPI.

Control factors	Level 1	Level 2	Level 3
Voltage	0.6266*	0.4549	0.4490
Electrolyte concentration	0.7205*	0.4281	0.3820
Wire feed velocity	0.4356	0.6211*	0.4739
Workpiece thickness	0.5056	0.4838	0.5412*

*Optimum parameter level

Table 13. Results of ANOVA on MPI.

Symbol	Control factors	DOF	SS	V	F value	PC (%)
A	Voltage	2	0.0610	0.0305	12.20	18.72
B	Electrolyte concentration	2	0.2022	0.1011	40.44	62.06
C	Wire feed velocity	2	0.0575	0.0288	11.52	17.68
D	Workpiece thickness	2	0.0050[#]	0.0025	-	01.54
Pooled error		2	0.0050	0.0025		
Total		8	0.3257	-		100

[#] Pooled error

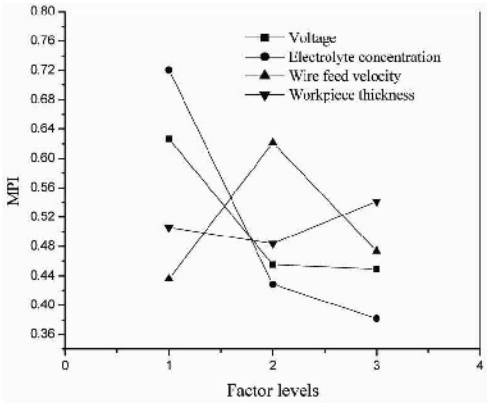

Fig. 8. Plot of average MPI values at different factor levels.

estimate quantitatively the relative significance (F-ratio), and also the percentage contribution (PC) of each factor on quality characteristics. The sum of squares (SS) and variance (V) for each factor, and pooled error (EP) obtained by pooling of factor D is calculated first, to evaluate the F value and PC. The ANOVA given in Table 13 shows the percentage contribution of different control factors on multiple quality characteristics (R_a and MRR) in ascending order as: workpiece thickness (1.54), wire feed velocity (17.68), voltage (18.72) and electrolyte concentration (62.06).

Therefore, the factors A and B are the most significant with respect to the MPI and they account for about 81% of the total variation in MPI. On the other hand, factor D has the smallest contribution and added to the pooled error. From the results of confirmation experiment (Table 14), the value of R_a and MRR at this optimum level are 4 μm and 0.5342 mm^3/min against the initial process parameter setting of 4.6 μm and 0.1658 mm^3/min. Hence, improvement in MRR by 222% and reduction in R_a by 15% have been found while machining at the optimum parameter setting against initial parameter setting. Table 15 shows the optimum quality values of R_a and MRR found from Taguchi methodology (i.e. R_a = 4.4 μm and MRR = 0.3647 mm^3/min) and hybrid methodology (i.e. R_a = 4 μm and MRR = 0.5342 mm^3/min). Finally, it has been obtained that MRR enhances by 46% and R_a reduces by 10% while the hybrid approach is applied.

Table 14. Results of confirmation experiment using TMWPC.

	Optimum values		
	Initial parameter setting	Prediction	Experiment
Level	$A_1B_1C_1D_1$	$A_1B_1C_2D_3$	$A_1B_1C_2D_3$
R_a (μm)	4.6	-	4
MRR (mm^3/min)	0.1658	-	0.5342

Table 15. Comparison of results of Taguchi approach and hybrid approach.

Quality characteristics	Optimization technique		Improvement (%)
	Taguchi approach	Hybrid approach	
R_a (μm)	4.4	4	10%
MRR (mm^3/min)	0.3647	0.5342	46%

6. Conclusions

In present study, hybrid TMRSM approach has been used for modeling and hybrid TMWPC approach is used for multi-objective optimization of TW-ECSM of rectangular borosilicate glass workpiece. Based on the modeling and optimization results, the following conclusions are summarized:

(1) The developed second-order response surface models for R_a and MRR using CCRD matrix have been found adequate. It has also been analysed from the results of regression coefficients that the linear effects of process parameters are significant for both the models.

(2) Electrolyte concentration, workpiece thickness, square effect of voltage and interaction effect of wire feed velocity and workpiece thickness have been obtained as the significant factors for R_a. The MRR has been found to be significantly affected by voltage, wire feed velocity, square effect of workpiece thickness and interaction effect of electrolyte concentration and workpiece thickness.

(3) From the response surface plot it has been observed that workpiece thickness has less effect on R_a as well as MRR compared to other process parameters. For achieving smaller value of R_a and larger value of MRR a higher value of wire feed velocity is required.

(4) From the Taguchi-based WPC, it has been found that the initial setting of TW-ECSM process parameters is most attractive for getting lower value of R_a and higher value of MRR out of 9 experiments. The application of TMWPC approach has reduced R_a by 15% and improved MRR by 222% from the initial value.

(5) It has been observed that in comparison to TM, the hybrid approach enhances MRR by 46% and reduces the R_a by 10%.

Acknowledgment

Authors would like to thank the Council of Scientific and

Industrial Research (CSIR), Government of India, New Delhi for providing the financial assistance for this experimental work of the project entitled "Experimental and Numerical Study of Traveling Wire Electrochemical Spark Machining of Advanced Engineering Materials" (Project no.: 22/0486/09-EMR-II).

References

[1] H. Kurafuji and K. Suda, Electrical discharge drilling of glass, *Annals of the CIRP,* 16 (1968) 415-419.

[2] R. Wuthrich and V. Fascio, Machining of non-conducting materials using electrochemical discharge phenomenon-an overview, *International Journal of Machine Tools & Manufacture,* 45 (9) (2005) 1095-1108.

[3] H. Tsuchiya, T. Inoue and M. Miyazaiki, Wire electrochemical discharge machining of glasses and ceramics, *Bulletin Japanese Society of Precision Engineering,* 19 (1) (1985) 73-74.

[4] I. Basak and A. Ghosh, Mechanism of spark generation during electrochemical discharge machining: a theoretical model and experimental investigation, *Journal of Material Processing Technology,* 62 (1) (1996) 46-53.

[5] H. El Hofy and J. A. McGeough, Evaluation of an apparatus for electrochemical arc wire-machining, *ASME Transaction Journal of Engineering for Industry,* 110 (2) (1988) 119-123.

[6] W. Y. Peng and Y. S. Liao, Study of electrochemical discharge machining technology for slicing non-conductive brittle materials, *Journal of Material Processing Technology,*149 (1-3) (2004) 363-369.

[7] V. V. Nesarikar, V. K. Jain and S. K. Choudhury, Traveling wire electrochemical spark machining of thick sheets of Kevlar-Epoxy composites, *Proc. of Sixteenth All India Manufacturing Technology Design and Research Conference, Bangalore, India* (1994) 672-677.

[8] V. K. Jain, P. S. Rao, S. K. Choudhury and K. P. Rajurkar, Experimental investigations into traveling wire electrochemical spark machining (TW-ECSM) of composites, *ASME Transaction Journal of Engineering for Industry,*113 (1) (1991) 75-84.

[9] C. T. Yang, S. L. Song, B. H. Yan and F. Y. Huang, Improving machining performance of wire electrochemical discharge machining by adding SiC abrasive to electrolyte, *International Journal of Machine Tools & Manufacture,* 46 (15) (2006) 2044-2050.

[10] Y. P. Singh, V. K. Jain, P. Kumar and D. C. Agrawal, Machining piezoelectric (PZT) ceramics using an electrochemical spark machining (ECSM) process, *Journal of Material Processing Technology,* 58 (1) (1996) 24-31.

[11] J. L. Lin, K. S. Wang, B. H. Yan and Y. S. Tarng, Optimization of the electrical discharge machining process based on the Taguchi method with fuzzy logics, *Journal of Material Processing Technology,*102 (1-3) (2000) 48-55.

[12] P. N. Singh, K. Raghukandan and B. C. Pai, Optimization by grey relational analysis of EDM parameters on machining Al-10%SiCP composites, *Journal of Material Processing Technology,* 155-156 (2004) 1658-1661.

[13] A. Sharma and V. Yadava, Modeling and optimization of cut quality during pulsed Nd: YAG laser cutting of thin Al-alloy sheet for straight profile, *Optics & Laser Technology,* 44 (1) (2012) 159-168.

[14] W. G. Cochran and G. M. Cox, *Experimental designs*, Asia Publishing House, Bombay (1959).

[15] M. S. Phadke, *Quality engineering using robust design*, Prentice-Hall, Englewood Cliffs, New Jersey, USA (1989).

[16] P. J. Ross, *Taguchi technique for quality engineering*, McGraw Hill, New York (1988).

[17] J. Antony, Simultaneous optimization of multiple quality characteristics in manufacturing processes using Taguchi's quality loss function, *International Journal of Advanced Manufacturing Technology,* 17 (2) (2001) 134-138.

[18] D. C. Montgomery, *Design and analysis of experiments*, John Wiley, New York (1997).

[19] H. C. Liao, Multi-response optimization using weighted principal component, *International Journal of Advanced Manufacturing Technology,* 27 (7-8) (2006) 720-725.

[20] S. K. Gauri and S. Chakraborty, Optimisation of multiple responses for WEDM processes using weighted principal components, *International Journal of Advanced Manufacturing Technology,* 40 (11-12) (2009) 1102-1110.

Basanta Kumar Bhuyan received his M.Tech from Moharshi Dayananda University, Rohtak, Haryana, India in 2008. He is currently pursuing his Ph.D. in the Department of Mechanical Engineering, Motilal Nehru National Institute of Technology Allahabad, Allahabad (India). His area of interest includes Conventional and Unconventional Machining Processes, Machining of Advanced Engineering Materials, Application of FEM and Design of Experiments in Manufacturing.

Vinod Yadava is currently a Professor in the Department of Mechanical Engineering and Dean (Research and Consultancy), Motilal Nehru National Institute of Technology Allahabad, Allahabad (India). He received his Ph.D. from Indian Institute of Technology Kanpur, (India) in 2002. His research area includes Advanced Manufacturing Science and Technology, Micromachining Science and Technology, Applications of Finite Element Method, Design of Experiments and Soft Computing Methods in Manufacturing.